Open Access Full Text Article

ORIGINAL RESEARCH

NaCl: for the safer in vivo use of antibacterial silver based nanoparticles

Mingzhuo Liu[1]
Huiqing Zhang[1]
Xiangwei Song[2]
Chaochao Wei[2]
Zhenfang Xiong[3]
Fen Yu[2]
Chen Li[4]
Fanrong Ai[5]
Guanghua Guo[1,*]
Xiaolei Wang[2,*]

[1]Department of Burns, The First Affiliated Hospital, Nanchang University, Nanchang, Jiangxi, China; [2]Department of Translational Medicine, Nanchang University, Nanchang, Jiangxi, China; [3]Department of Pathology, The First Affiliated Hospital, Nanchang University, Nanchang, Jiangxi, China; [4]Department of Orthopedic Surgery, The Second Affiliated Hospital of Nanchang University, Nanchang, Jiangxi, China; [5]School of Mechanical & Electronic Engineering, Nanchang University, Nanchang, Jiangxi, China

*These authors contributed equally to this work

Correspondence: Guanghua Guo
Department of Burns, The First Affiliated Hospital, Nanchang University, 17 Yongwai Street, Donghu District, Nanchang 330006, China
Tel +86 130 0722 2375
Email guoghtg@sina.com

Xiaolei Wang
Department of Translational Medicine, Nanchang University, 1299 Xuefudadao, Honggu District, Nanchang 330088, China
Tel +86 186 7985 0415
Email wangxiaolei@ncu.edu.cn

Background: As antibiotics progressively cease to be effective, silver based nanoparticles (SBNs), with broad antibacterial spectrum, might be the last line of defense against malicious bacteria. Unfortunately, there are still no proper SBNs-based strategies for in vivo antibacterial therapies. In this article, new carbon membrane packaged Ag nanoparticles (Ag-C) were synthesized. We assessed the effect of Ag-C with NaCl on size, cytotoxicity, antibacterial properties, metabolism and sepsis models.

Methods: The size of Ag-C with NaCl was accessed with UV-vis, TEM and SEM. *Staphylococcus aureus*, *Escherichia coli* and *Pseudomonas aeruginosa* were used to illustrate the antibacterial properties of SBNs affected by NaCl. L929 and 3T3 cell lines were cultured in vitro; CCK-8 assay was used to test cytotoxicity. Then, we explored the metabolism of Ag-C with NaCl in vivo. Finally, the effect of Ag-C with 4× NaCl on sepsis was observed.

Results: NaCl could regulate the size of Ag-C. Ag-C exhibited superior antibacterial properties compared to similar sized pure Ag nanoparticles. Furthermore, the addition of NaCl could not only reduce the cytotoxicity of Ag-C, but could also continue to discharge Ag-C from major organs. Based on these factors, this method was used to treat a sepsis model (induced via cecal ligation and puncture), and it achieved satisfactory survival results.

Conclusion: This discovery, though still in its infancy, could significantly improve the safety and feasibility of SBNs and could potentially play an important role in modern in vivo antibacterial applications. Thus, a new method to combating the growing threat from drug-resistant bacteria could be possible. NaCl is the key to excretion of SBNs after in vivo antibacterial use.

Keywords: Ag nanoparticles, NaCl, cytotoxicity, antibacterial, metabolism

Introduction

Since the discovery of penicillin in 1928, antibiotics have gradually become one of the bases of modern health care by saving billions of patients around the world.[1] However, with the misuse of antibiotics in clinics and animal husbandry, many bacteria have evolved in the past nearly 90 years, they are no longer sensitive to antibiotics and have caused bacterial resistance worldwide.[2–5] People will be forced to face a devastating reality, which is the post-antibiotics era, where most cures become futile. To solve this problem, the general public, medical practitioners, policy makers, and pharmaceutical companies are called upon to find a solution for this crisis.[6,7] Currently, the present methods are only able to delay the occurrence of antibiotic resistance. No solution has been found to fundamentally eliminate the problem indefinitely.[8,9] Therefore, new antibacterial concepts are desperately needed to solve the current bacterial resistance problem. One suggestion is to develop an effective and safe antibiotic substitute.[10,11]

Nano-science and technology is an emerging field with a lasting impact on medical science.[12,13] Owing to their excellent broad-spectrum antibacterial property, various

silver based nanoparticles (SBNs) have been used extensively in vitro in antibacterial fields.[14–17] In theory, SBNs might also have an inhibitory effect on pathogens in vivo, including some drug-resistant strains. If the safe use of SBNs in the body was guaranteed, it might be able to replace some existing antibiotics.[18,19] By these means, bacteremia, skin infections, bacterial meningitis, and other related diseases could have new treatments. However, to our knowledge, surprisingly few studies are focused on the in vivo applications of SBNs. The reality is that people are still concerned about the safety of long-term use of SBNs in vivo,[20,21] which may damage organs and tissues.[22–25] Therefore, a group of volunteers are urgently needed to conduct a thorough study on these unclear areas and find a safer way to use SBNs in vivo, which is the premise of ensuring effective antibiotics and minimized side effects to internal organs.

In the previous study,[26] we found that the use of different concentrations of PBS solution could trigger the three modes of transformation of carbon membrane packaged Ag nanoparticles (Ag-C), ie, the packaging, the activation, and the deactivation. Therefore, the purpose of controlling the antibacterial activities of SBNs could be achieved. However, its detailed mechanism is not certain at the moment as there is no guarantee that this same adjustment could also be realized in the in vivo situation. In a combined effort based on other teams' former investigations,[26–28] a new kind of Ag-C was firstly synthesized, after which we investigated how to adjust the mode, switching from activation to aggregation more effectively. The metabolism of the obtained SBNs was also discussed in in vivo applications of this mode switch.

Materials and methods
Materials
Potassium sodium tartrate tetrahydrate (PSTT) and AgNO₃ were purchased from Sinopharm Chemical Reagent Co. Ltd (Shanghai, China). *Staphylococcus aureus* (American Type Culture Collection, Manassas, VA, USA [ATCC] 25923), *Escherichia coli* (ATCC 25922), and *Pseudomonas aeruginosa* (ATCC 10145) were purchased from ATCC. L929 and 3T3 cells were also purchased from ATCC.

Preparation of the carbon dots (CDs)
The CDs were synthesized by pyrolysis of PSTT, according to Liu's report.[26] Briefly, 3.03 g PSTT was prepared in a tube furnace at 400°C for 6 h at a heating rate of 10°C/min under an N₂ atmosphere. Once the product cooled to room temperature, it was dispersed in 80 mL deionized water in the dark, ultrasound dispersed (700 W) for 60 min, and centrifuged at 9,500 rpm/min for 16 min to remove large, insoluble particles. Then, the brown supernatant liquid was collected and heated at 80°C for less than 2 h until 60 mL liquid had evaporated. An amount of 60 mL acetone was added, it was ultrasound dispersed (700 W) for 30 min, and centrifuged at 9,500 rpm/min for 16 min. Finally, the supernatant liquid was collected, which was the original carbon dots and transferred to the original CDs.

Preparation of Ag-C and Ag solution
An amount of 25 mL CDs liquid was diluted to 100 mL with deionized water and adjusted to pH 7 with concentrated ammonia, followed by ultra-sonication for 20 min. Freshly prepared Tollen's stock solution was obtained.[29] An amount of 1 mL fresh Tollen's reagent was added into the 100 mL solution, which was heated at 120°C and stirred at 500 rpm/min under reflux, which lasted for less than 20 min. Subsequently, the final product, consisting of yellow Ag-C solution, was obtained. An amount of 25 mL acetone was diluted to 100 mL with deionized water. The next procedure was similar to that described previously.

Obtained Ag-C or Ag solution was examined by transmission electron microscopy (TEM) (JEM-2100; JEOL, Tokyo, Japan), ultraviolet (UV)-visible (vis) absorption spectra (UV-2600; Shimadzu Corporation, Kyoto, Japan), scanning electron microscopy (SEM) (Sigma 300; Carl Zeiss Meditec AG, Jena, Germany), and zeta potential (90Plus PALS, Brookhaven Instruments Corporation, Holtsville, NY, USA).

Preparation of PBS, NaCl, K₂HPO₄, and KCl
The 1× PBS solution contained the following: 137 mM NaCl, 2.7 mM KCl, 10 mM Na_2PO_4, and 1.8 mM KH_2PO_4. So the concentration of Na^+, K^+ and PO_4^{3-} was 157 mM, 74.55 mM, and 11.8 mM respectively.

We used these molar concentrations as formula preparation in terms of NaCl, KCl, and $K_2H\,PO_4$. Consequently, 1× PBS solution contained 9.18 g NaCl, 0.34 g KCL, and 2.69 g $K_2H\,PO_4$. The pH was adjusted to 7.4 with HCl, then, H_2O was added to 1 L. PBS 10× stock was diluted to 8×, 4×, and 2×, so it was the same as NaCl, KCl, and $K_2H\,PO_4$.

Antibacterial properties assay in vitro
S. aureus (ATCC 25923), *E. coli* (ATCC 25922), and *P. aeruginosa* (ATCC 10145) were chosen to assess the antibacterial ability of Ag-C or Ag with 10× NaCl. These were cultured in Luria-Bertani broth at 37°C for 24 h; 100 µL bacterial stock solution with Ag-C or Ag with 10× NaCl was added to 5 mL Luria-Bertani broth and incubated in an orbital shaker at 37°C for 3 h. After that, 100 µL co-culture medium was serially diluted 1×10⁵ times with PBS and

50 µL of the diluents was used to spread on the solid LB agar coated on the petri dishes, which were placed in a constant 37°C temperature incubator for 24 h. Then, the colonies were formed. The inhibition rate (IR) was determined by distinguishing the number of colony forming units (CFU). The IR was based on the following formula:

$$IR = \frac{C - Cx}{C} \times 100\%$$

where Cx was the number of the experimental group's CFU after treatment with Ag-C or Ag with 10× NaCl, on diverse bacteria, and C was the number of bacteria in the control group.

Cytotoxicity

L929 and 3T3 cells were cultured in DMEM (GE, Boston, MA, USA) with 10% fetal bovine serum (Thermo Fisher Scientific, Waltham, MA, USA) and 1% penicillin/streptomycin in a humidified incubator at 37°C under an atmosphere of 5% CO_2, and the culture medium was replaced every day. Cells (1×10^4) were seeded in 96-well plates after being digested by trypsin until the cells attached to the wells. An amount of 10 µL Ag-C or Ag with different concentrations of NaCl was added to each well of the 96-well plates when the culture medium was replaced. After incubation for 6 h, 24 h, and 7 d, all the media were removed by pipette and 100 µL fresh media and 10 µL Cell Counting Kit (CCK)-8 reagent (Dojindo, Kyushu, Japan) were added to the cell culture dish, followed by an additional 1 h incubation at 37°C. Afterwards, a microplate reader (SpectraMax M5; Molecular Devices LLC, Sunnyvale, CA, USA) was used to measure the optical density (OD) at a wavelength of 450 nm. The cell viability (%) was calculated as follows:

$$\text{Cell viability (\%)} = \frac{\text{OD 450 nm in test cells}}{\text{OD 450 nm in control cells}} \times 100\%.$$

Animal model

All experiments were performed in compliance with the relevant laws and approved by the Institutional Animal Care and Use Committee at Institute of Translational Medicine, Nanchang University. All mice were fed with a standard diet and housed in a ventilated room maintained at 26°C and 70% relative humidity, and with a 12 h light and dark cycle. All animal handling procedures were performed according to the Guide for the Care and Use of Laboratory Animals of the Chinese Association for Laboratory Animal Sciences and followed the guidelines of the Animal Welfare Act. Male Kunming (KM) mice were purchased from the medical laboratory of Animal Science of Nanchang University.

Mice metabolism

Six-week old healthy male KM mice with body weight ranging from 20 g to 25 g were selected. The mice were completely randomly divided into five groups (n=4): sham group, Ag-C group, Ag-C+1×H₂O group, Ag-C+1×NaCl group, Ag-C+4×NaCl group, and Ag-C+10×NaCl group. Experimental mice were continuously intra-peritoneally injected with the same concentration of Ag-C at 100 µL/ 10 g dose every 12 h for 7 d and deionized water or different concentrations of NaCl at 100 µL/10 g level every 12 h for 14 d. The sham group was punctured every 12 h by the same 25-gauge needle. Body weight was recorded every day. On the last day, the mice were sacrificed and organs were retrieved for inductively coupled plasma mass spectrometry (Optima8000, PerkinElmer Inc., Waltham, MA, USA) tests.

In vivo sepsis studies

Nine-week old healthy male KM mice with body weight ranging from 35 g to 38 g were selected. The mice were completely randomly divided into four groups (n=8): sham group, sepsis group, sepsis+Ag-C group, and sepsis+Ag-C+4×NaCl group. Pre-operatively, mice were anesthetized by intra-peritoneal injection of 10% (w/w) chloral hydrate (0.005 mL/g). A high-grade sepsis model was created by cecal ligation and puncture (CLP), using the same 21-gauge needle, as per Rittirsch et al's work.[30] Experimental mice were continuously intra-peritoneally injected with the same concentration of Ag-C at 100 µL/10 g dose every 12 h for 7 d and sterile water or 4× NaCl at 100 µL/10 g level every 12 h for 14 d. The sham group underwent the following procedures: dissection of the abdomen only, and caecum located after shaving and cleaning the abdomen skin. After the operation, mice were resuscitated by injecting pre-warmed normal saline (37°C; 50 µL/g body weight) subcutaneously. Body weight was recorded every day. On the last day, the mice were sacrificed, organs were retrieved for hematoxylin-eosin staining, fixed, embedded and cut into 5 mm serial sections, and finally stained. Histological sections were examined under an Olympus BX41 microscope equipped with digital camera for capturing images.

Statistical analysis

Statistical data are expressed as the means ± SD. The experiments were conducted three or four times. Differences between mean values were analyzed with one-way analysis of variance (ANOVA) followed by Tukey test for multiple comparisons. The non-parametric analysis

followed by independent sample Kruskal–Wallis test was applied to determine the level of significance, instead of a standard one-way ANOVA, when these data were from a suspected non-normal population. The survival difference between groups was analyzed by the log-rank (Mantel-Cox) test. Significance was considered for p-value <0.05 or p-value <0.01.

Results

Comparison between Ag-C and Ag

As shown in Figure 1A–C, the average size of normal Ag was 12.76 ± 4.13 nm. On the other hand, Figure 1D–F shows the well mono-dispersed SBNs synthesized by carbon quantum dots (CQD) with an average size of 13.23 ± 4.03 nm, the size of which was almost equal to the former naked Ag.

UV-vis absorption spectra of Ag-C with PBS, NaCl, K_2HPO_4, and KCl

UV-vis absorption spectra results showed that Ag-C absorbance wavelength was 422 nm and only the peak spectrum of Ag-C caused by NaCl (Figure 2B) was similar to that of PBS (Figure 2A). Compared with KCl, K_2HPO_4 (Figure 2C and D), NaCl had the same color change as the Ag-C affected by PBS.

SEM and zeta potentials of Ag-C with PBS, NaCl, K_2HPO_4, and KCl

As shown in Figure 3A–L, with the increase of NaCl concentration, Ag-C aggregation became increasingly apparent.

It is worth mentioning that when NaCl was added ×8, the average size of Ag-C increased, but the entire dispersion barely changed, only occasionally large aggregated clusters appeared. However, when the NaCl concentration increased to ×10, the number of aggregated Ag-C (>1 µm in diameter) was significantly increased, which became the principal form of Ag-C. As shown in Table S1, zeta potentials of Ag-C with increasing NaCl became lower.

Antibacterial properties

Ag-C's antibacterial properties on the Gram-positive *S. aureus* (ATCC 25923) and the Gram-negative *E. coli* (ATCC 25922) were slightly better than the normal Ag (Figure 4A–J). To clearly illustrate the antimicrobial action of SBNs affected by NaCl, 10× NaCl was used. After adding 10× NaCl, the antibacterial effect of Ag-C was significantly reduced ($72.59\%\pm17.57\%$ vs $15.06\%\pm19.66\%$, $p=0.005$ for *S. aureus* and $79.56\%\pm10.50\%$ vs $15.86\%\pm20.34\%$, $p=0.035$ for *E. coli*), due to its apparent aggregation, as shown in Figures 3K and 4K. However, the aggregation of Ag-C and Ag still presented a strong antibacterial effect on the *P. aeruginosa* (ATCC 10145), as shown in Figure S1.

Cytotoxicity

As shown in Figure 5A and B, Ag-C exhibited excellent cell compatibility in a relatively short time. L929 co-cultured with Ag-C for 7 d, adding 4×, 8×, and 10× NaCl did not show any obvious toxicity. As a matter of fact, these groups even promoted cell proliferation effectively (Figure 5C), compared with Ag-C ($93.80\%\pm27.02\%$ vs $124.42\%\pm16.95\%$,
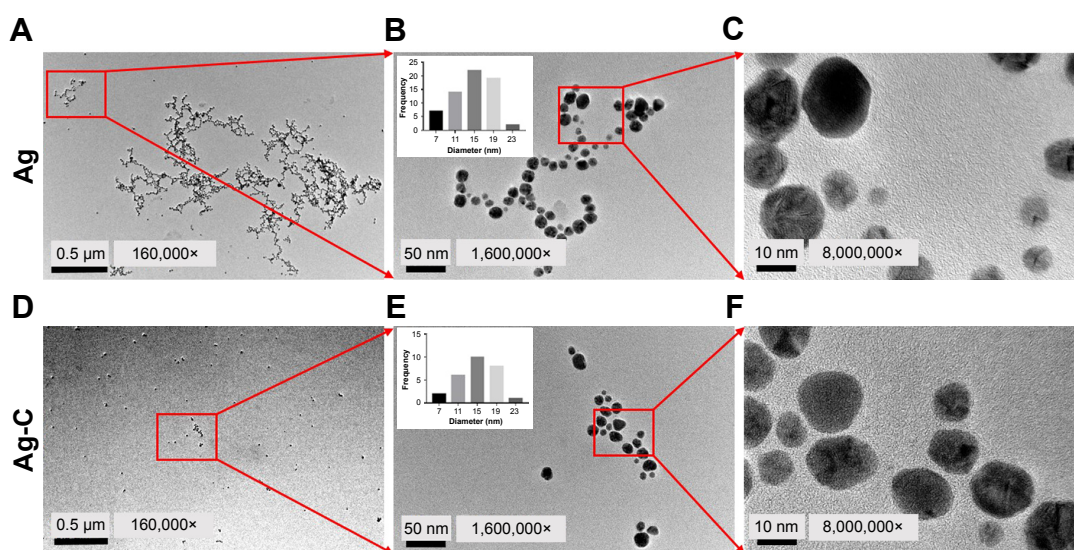
Figure 1 TEM images of normal Ag (**A–C**) and Ag-C (**D–F**). The insert is the average size of nano-silver.
Abbreviations: TEM, transmission electron microscopy; Ag-C, carbon membrane packaged Ag nanoparticles.
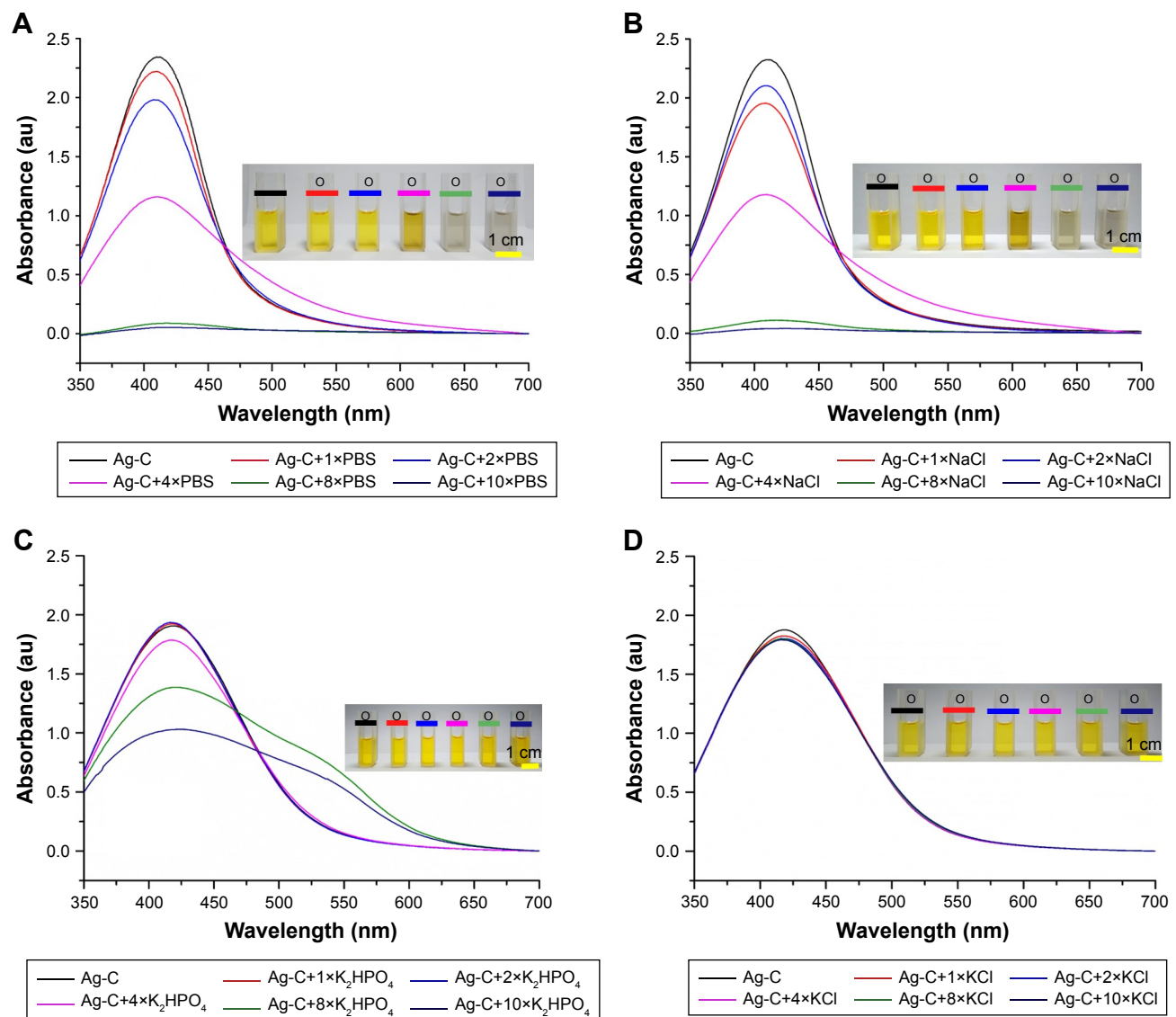
Figure 2 Ultraviolet-visible absorption spectra of Ag-C with different concentrations of PBS and containing NaCl, K_2HPO_4, and KCl (**A–D**).
**Note:** Inset: photographs of the related visible changes of Ag-C solution (2 mL) in the presence of the same volume (100 μL) and different concentrations of PBS and containing NaCl, K_2HPO_4, and KCl.
Abbreviation: Ag-C, carbon membrane packaged Ag nanoparticles.

p=0.04 for 4×; 93.80%±27.02% vs 121.22%±19.15%, p=0.08 for 8×; 93.80%±27.02% vs 119.71%±16.13%, p=0.01 for 10×) and Ag-C combined with 1× NaCl (94.58%±5.10% vs 124.42.75%±16.95%, p=0.07 for 4×; 94.58%±5.10% vs 121.22%±19.15%, p=0.015 for 8×, and 94.58%±5.10% vs 119.71%±16.13%, p=0.018 for 10×). Furthermore, 3T3 cells were also used and a similar phenomenon was found (Figure 5D and E). Ag-C with 4× or more NaCl could promote cell proliferation more effectively than the control group (Figure 5F), and the results were statistically significant (100.00%±00.00% vs 150.62%±16.95%, p=0.015 for 4×; 100.00%±00.00% vs 149.72%±18.54%, p=0.017 for 8×, and 100.00%±00.00% vs 149.79%±17.33%, p=0.017 for 10×).

Animal metabolism

The primary objective of this study was to explore as to whether NaCl could regulate the metabolism of Ag-C in vivo. Twenty mice were thus divided into five groups, injecting the relative dose (100 μL/10 g) of Ag-C for 5 d and different doses of NaCl for 14 d. Inductively coupled plasma mass spectrometry was then employed to analyze the Ag and Na concentration in the three main metabolic organs (liver, spleen, and kidney). Results illustrated that after injecting the Ag-C alone, only the Ag content in the liver and kidney was increased (Figure 6A–C). After injecting the 1× or 4× NaCl, the content of Ag in the three organs could be further reduced. However, it is worth noting that, if too much NaCl (10×) was added,
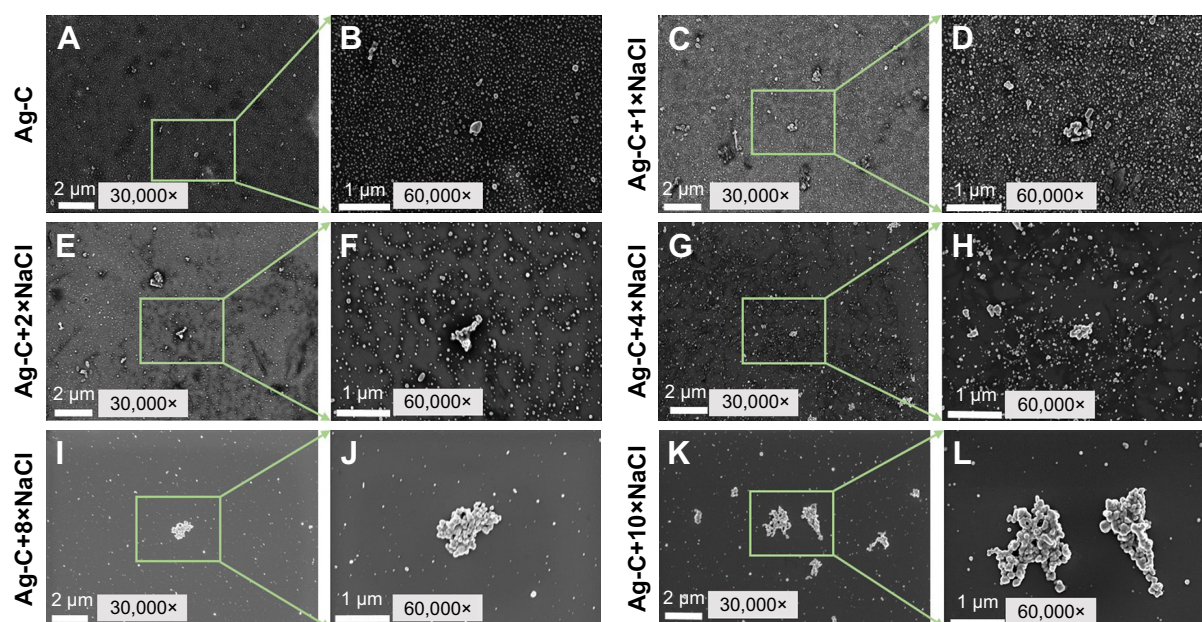
Figure 3 SEM images of the 2 mL Ag-C (**A–L**) with 200 μL different concentrations of NaCl.
Abbreviations: SEM, scanning electron microscopy; Ag-C, carbon membrane packaged Ag nanoparticles.
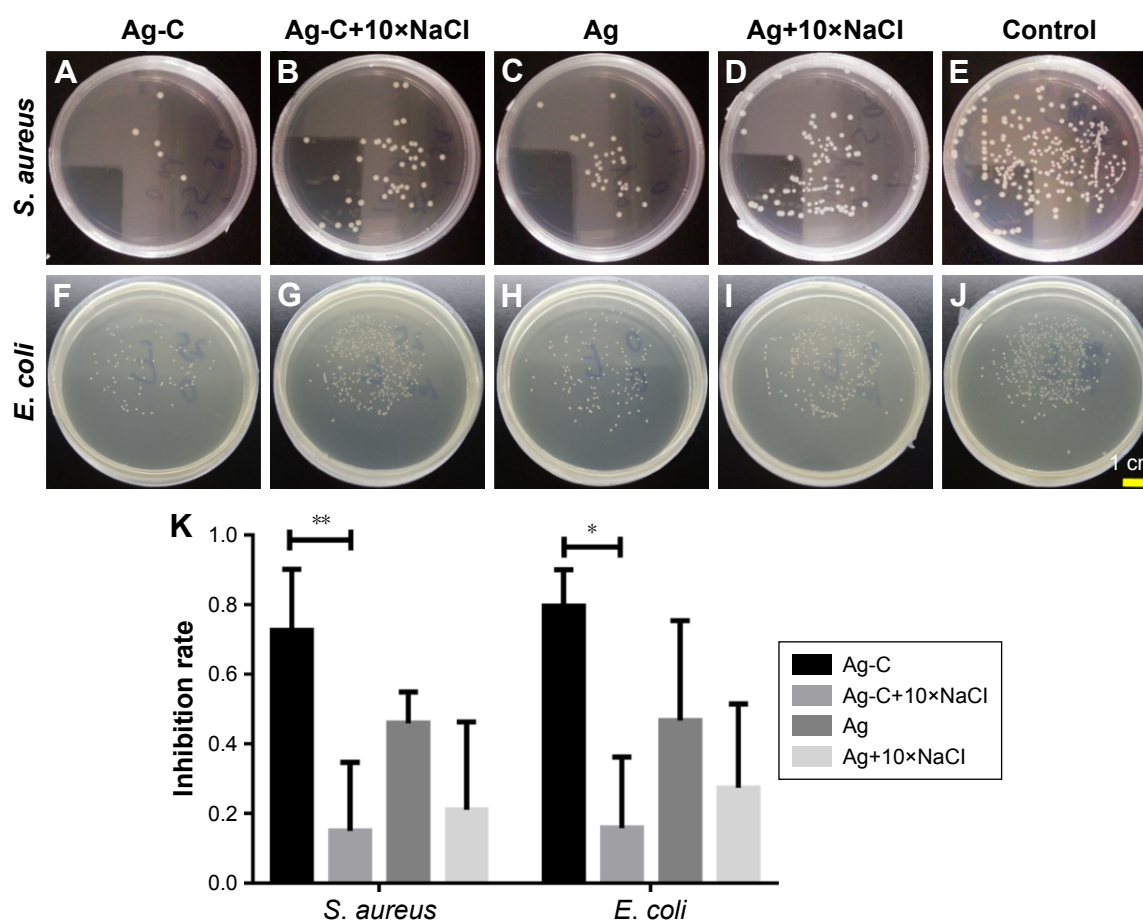

Figure 4 Plate counting photographs of Gram-negative *Escherichia coli* and Gram-positive *Staphylococcus aureus* co-cultured with Ag-C and Ag or with 10× NaCl in vitro for 3 h (**A–J**).
Notes: The corresponding inhibition rates of bacteria (**K**). **$p<0.01$ and *$p<0.05$ vs Ag-C+10×NaCl. Differences between mean values were analyzed with one-way ANOVA followed by Tukey test for multiple comparisons.
Abbreviations: Ag-C, carbon membrane packaged Ag nanoparticles; ANOVA, analysis of variance.
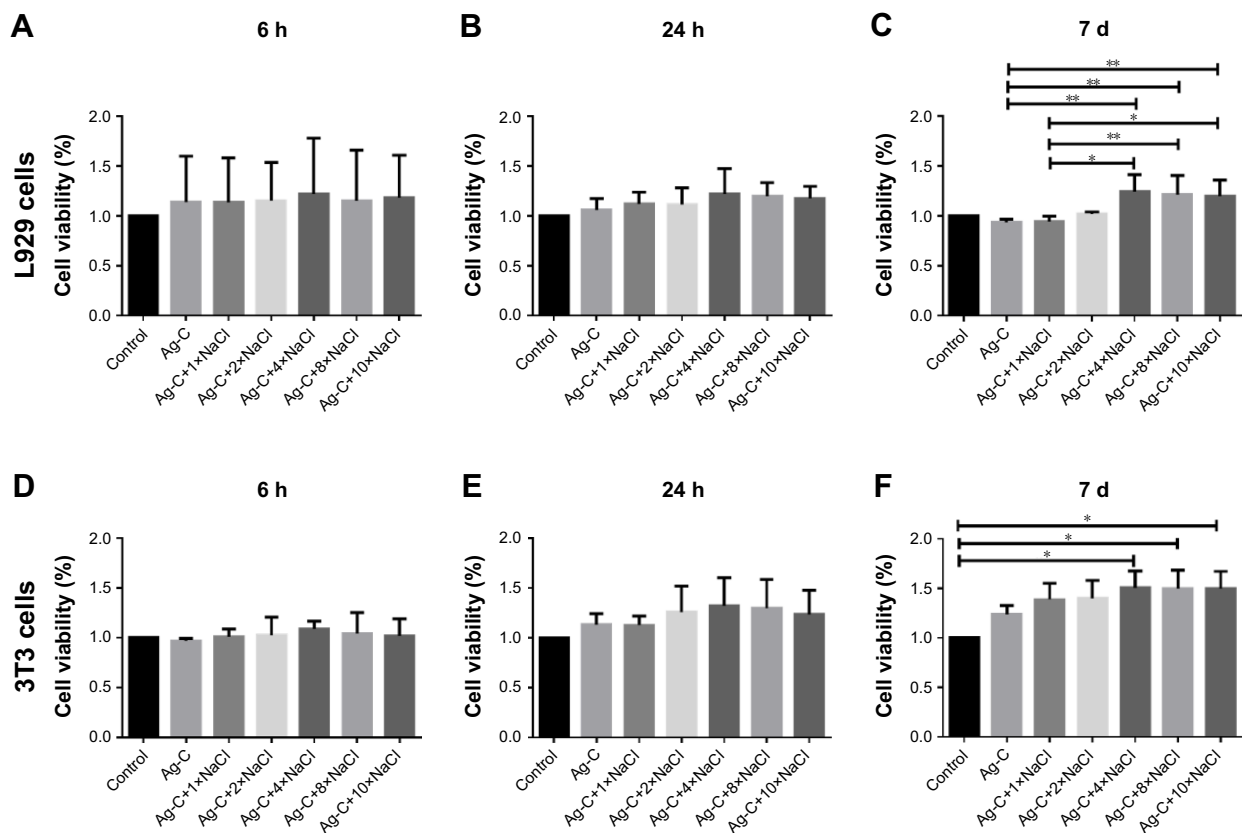
Figure 5 Cell biocompatibility of Ag-C under different NaCl concentrations at 6 h, 24 h, and 7 d.
Notes: $**p < 0.01$, $*p < 0.05$. There are no significance in L929 or 3T3 test at 6 h and 24 h (**A**, **B** and **D**, **E**). Differences in L929 test among groups were analyzed with non-parametric analysis followed by independent sample Kruskal–Wallis test instead of a standard one-way ANOVA when these data were from a suspected non-normal population (**C**). Differences in 3T3 test among groups were analyzed with one-way ANOVA followed by Tukey test for multiple comparisons (**F**).
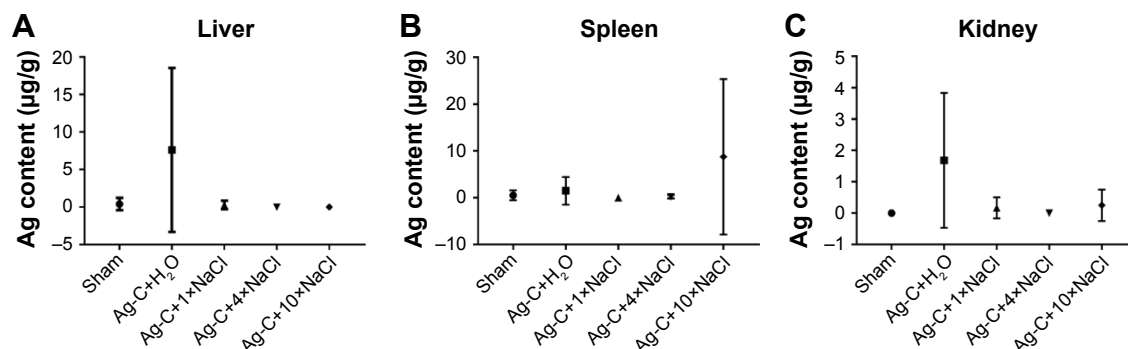**Abbreviations:** Ag-C, carbon membrane packaged Ag nanoparticles; ANOVA, analysis of variance.

Ag content became enriched in the spleen. This experiment had been repeated several times and similar results were obtained. Another interesting result demonstrated that Ag-C with different concentrations of NaCl did not lead to significant change in body and organ weight or Na concentrations in organs (Figures S2 A–G). These experimental results showed that at both the cellular level and in organ metabolism, 4×

NaCl was the ideal dose to adjust the Ag-C size and metabolism. Therefore, this concentration was chosen to proceed to the next stage of the experiment.

Sepsis model

Finally, as a practical application, the effect of Ag-C and 4× NaCl on sepsis was observed. From the results of hematoxy-

Figure 6 The average content of the injected Ag-C of total mice (n=4) in liver, spleen and kidney was analyzed (**A–C**).
Abbreviation: Ag-C, carbon membrane packaged Ag nanoparticles.

lin-eosin staining, the sepsis+Ag-C+4×NaCl group showed amelioration of inflammation of the heart, liver, spleen, lungs, and kidney, compared with the sepsis and sepsis+Ag groups (Figure 7A–T). The most frequently used CLP mice model was used in our experiments (Figure S3A–E). In the high-grade sepsis model, all mice in the sepsis group died 3 d after CLP (median survival time [MST] was 2.5 d). When using Ag-C injection alone, the treatment did not improve MST (1.5 d), but it could slow down the rate of death. At the same time, Ag-C combined with 4× NaCl could increse the MST (4.5 d) of this group (Figure 7U, p=0.0083).

Discussion

As shown in Figure 1A–F, with the help of CQD, the dispersion of Ag-C was significantly improved. In previous work, it was found that when PBS existed in vitro, Ag-C could effectively switch from the monodispersed to the aggregated mode.[26] In this work, in order to achieve effective switch and rapid metabolism of Ag-C material in vivo, the metal salts in PBS triggering the switch were studied. The three main components of PBS, which are NaCl, KCl, and K_2HPO_4, were mixed with Ag-C and then the UV-vis absorption spectra were measured. Results showed that NaCl played a leading role in the aggregation of Ag-C. It is a very intriguing discovery because NaCl is the most common metal salt for daily intake, compared with KCl, K_2HPO_4, and many other salts. Additionally, NaCl has a relatively high biological safety. Therefore, in terms of cost as well as safety, if NaCl could regulate the body's metabolism of Ag-containing antimicrobial agents, it would be an ideal choice and easy to promote.

To further confirm this discovery, morphology and size changes of Ag-C with different concentrations of NaCl were observed through SEM. As shown in Figure 3A–L, the results of SEM agreed with the data from UV-vis. The change of NaCl concentration affects the aggregation of Ag-C, so its corresponding performance might also be changed significantly. Apart from the size regulation, NaCl also changed the biological activity of Ag-C. To examine antibacterial properties', the Gram-positive *S. aureus* and the Gram-negative *E. coli* as well as *P. aeruginosa* were chosen as model strains. The results indicated that the addition of NaCl attributed to the change in the biological properties of Ag-C, except *P. aeruginosa*. An interesting phenomenon was that by adding 10× NaCl to the original Ag, this mixture could also reduce antibacterial properties, which was similar to the effect of Ag-C, but did not show a significant statistical difference.

As for changes in antibacterial properties, the work was mainly focused on the bio-compatibility of Ag-C before and after adding NaCl. L929 cells and 3T3 cells were selected as the cell line models to investigate the cytotoxicity of Ag-C with different NaCl concentrations at 6 h, 24 h, and 7d time points respectively. The two sets of data from cell experiments demonstrated that 4× NaCl or more could adjust the size of Ag-C, and exhibited high cell compatibility. Another phenomenon was found: a low concentration of SBNs could promote cell proliferation, and a high concentration is toxic. Previous work and related literature further confirmed this conclusion.[16,31,32] Collectively, the modification of carbon membrane could make the Ag nanoparticles more biocompatible and stable.[31] More importantly, the antibacterial properties of these nanocomposites were also improved compared to the similar sized bare Ag nanoparticles.[26]

These experimental results showed that 4× NaCl was the ideal dose to adjust Ag-C size and metabolism. However, the detailed mechanism remains to be further explored. For practical applications, the sepsis experiments used proved that Ag-C with broad-spectrum antibacterial properties indeed inhibited serious sepsis. The addition of 4×NaCl could effectively reduce the toxicity of Ag-C; this kind of method could lead to a better result, and may complement Kwok et al's work.[28] Yet, a bad result was that there were two mice alive in each group at the end of the experiment, except in the sham group. Although this was a proof of concept test, the results proved that using NaCl, playing good performances in antibacterial, cellar biocompatibility, tissue metabolism as well as pathology and practical therapy, could enhance the safe use of Ag-C. It is worth noting that this method could actually improve the MST of mice, but could not improve their survival rate. In the future, the therapeutic strategy needs to be more systemically optimized.

Conclusion

In recent years, therapy for infections has become much less effective due to the widespread dissemination of drug-resistant bacteria. With broad-spectrum antibacterial properties and excellent performance, SBNs, under extreme circumstances, could be a reliable alternative to conventional antibiotics. Unfortunately, until now, few papers relating to in vivo medical application of SBNs have been published.[15] One of the main reasons is the lack of safe methods for the in vivo use of SBNs. In this work, a method was discovered and proved that using Ag-C with NaCl. Even when Ag-C was injected into mice, most of this material did not accumulate in the metabolic organs. The most important finding was that with the addition of ×4 NaCl, the cell cytotoxicity of Ag-C could be further reduced by accelerating Ag-C metabolism. Consequently, satisfactory survival results were obtained for
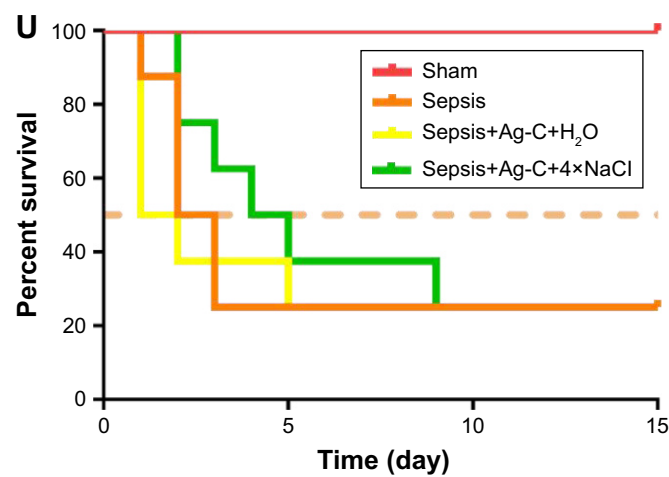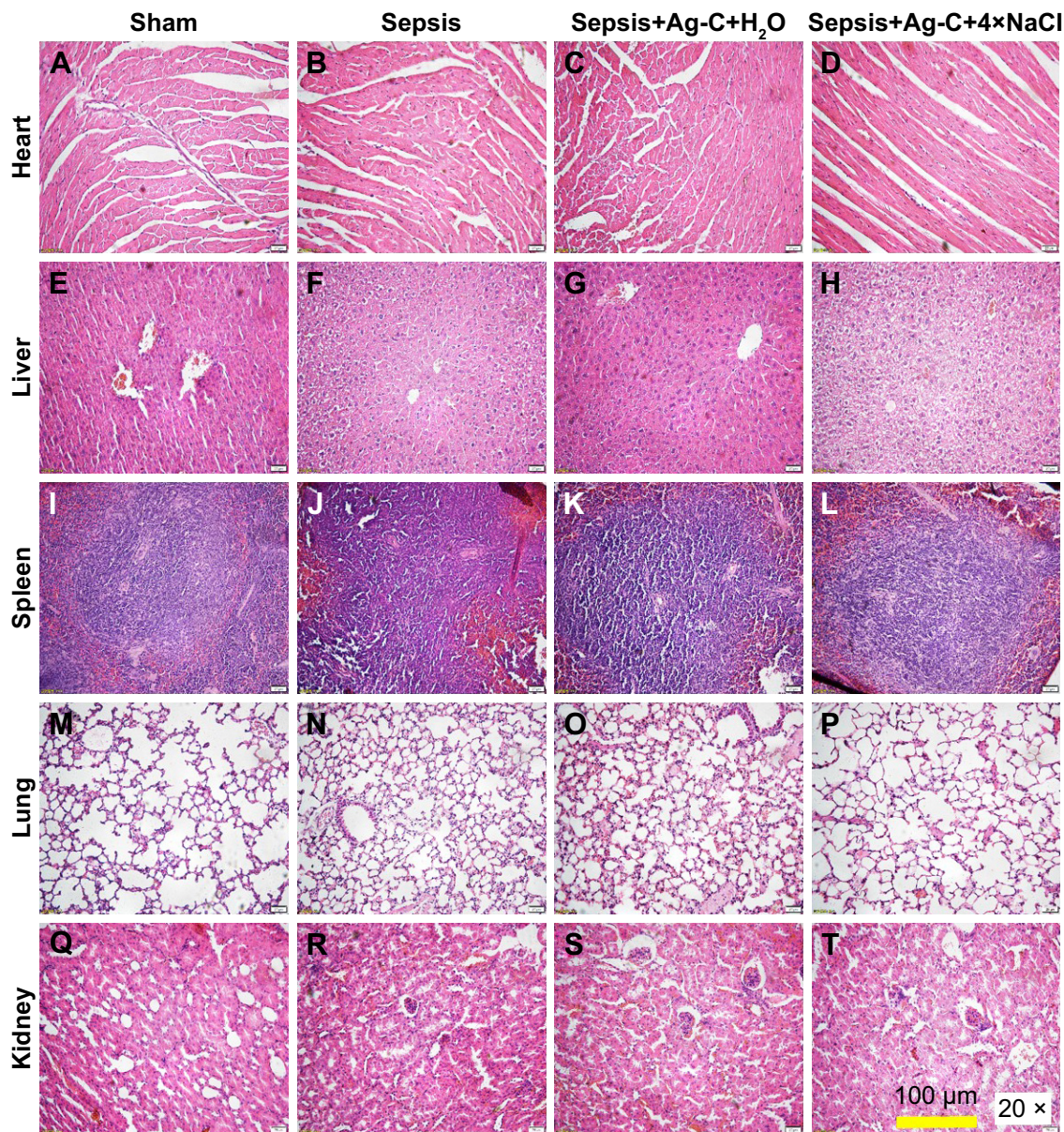
Figure 7 Pathological changes of mice that survived 15 d after CLP.
Notes: Heart, liver, spleen, lung, and kidney were stained by the hematoxylin-eosin method (**A–T**). Survival curves of different groups after CLP (**U**). The difference between groups was analyzed by the log-rank (Mantel-Cox) test.
Abbreviations: Ag-C, carbon membrane packaged Ag nanoparticles; CLP, cecal ligation and puncture.

the treatment of the high-grade sepsis model. Though this discovery is still in its infancy, it could potentially improve the safety and feasibility of SBNs significantly for in vivo antibacterial applications, which would provide a new method to combat the gradually growing threat from drug-resistant bacteria.

Acknowledgments

Disclosure

The authors report no conflicts of interest in this work.

References

1. Morrill HJ, Caffrey AR, Jump RL, Dosa D, LaPlante KL. Antimicrobial stewardship in long-term care facilities: a call to action. *J Am Med Dir Assoc*. 2016;17(2):183.e1–e16.
2. Arias CA, Murray BE. Antibiotic-resistant bugs in the 21st century – a clinical super-challenge. *N Engl J Med*. 2009;360(5):439–443.
3. Shankar PR. Antimicrobial resistance: global report on surveillance. *Australasian Medical Journal*. 2014;7(4):237.
4. Ventola CL. The antibiotic resistance crisis: part 1: causes and threats. *P T*. 2015;40(4):277–283.
5. Zhang QQ, Ying GG, Pan CG, Liu YS, Zhao JL. Comprehensive evaluation of antibiotics emission and fate in the river basins of China: source analysis, multimedia modeling, and linkage to bacterial resistance. *Environ Sci Technol*. 2015;49(11):6772–6782.
6. Ventola CL. The antibiotic resistance crisis: part 2: management strategies and new agents. *P T*. 2015;40(5):344–352.
7. Tang Q, Song P, Li J, Kong F, Sun L, Xu L. Control of antibiotic resistance in China must not be delayed: the current state of resistance and policy suggestions for the government, medical facilities, and patients. *Biosci Trends*. 2016;10(1):1–6.
8. Davies J, Davies D. Origins and evolution of antibiotic resistance. *Microbiol Mol Biol Rev*. 2010;74(3):417–433.
9. Zhuk I, Jariwala F, Attygalle AB, Wu Y, Libera MR, Sukhishvili SA. Self-defensive layer-by-layer films with bacteria-triggered antibiotic release. *ACS Nano*. 2014;8(8):7733–7745.
10. Bai H, Yuan H, Nie C, et al. A supramolecular antibiotic switch for antibacterial regulation. *Angew Chem Int Ed Engl*. 2015;54(45):13208–13213.
11. Richter AP, Brown JS, Bharti B, et al. An environmentally benign antimicrobial nanoparticle based on a silver-infused lignin core. *Nat Nanotechnol*. 2015;10(9):817–823.
12. Jha RK, Jha PK, Koel C, Rana SVS, Guha SK. An emerging interface between life science and nanotechnology: present status and prospects of reproductive healthcare aided by nano-biotechnology. *Nano Rev*. 2014;5:10.3402/nano.v5.22762.
13. Björnmalm M, Faria M, Caruso F. Increasing the impact of materials in and beyond bio-nano science. *Journal of the American Chemical Society*. 2016;138(41):13449–13456.
14. Song J, Kang H, Lee C, Hwang SH, Jang J. Aqueous synthesis of silver nanoparticle embedded cationic polymer nanofibers and their antibacterial activity. *ACS Appl Mater Interfaces*. 2012;4(1):460–465.
15. Chernousova S, Epple M. Silver as antibacterial agent: ion, nanoparticle, and metal. *Angew Chem Int Ed Engl*. 2013;52(6):1636–1653.
16. Xue C, Song X, Liu M, et al. A highly efficient, low-toxic, wide-spectrum antibacterial coating designed for 3D printed implants with tailorable release properties. *J Mater Chem B*. 2017;22.
17. Zhao R, Lv M, Li Y, et al. Stable nanocomposite based on PEGylated and silver nanoparticles loaded graphene oxide for long-term antibacterial activity. *ACS Appl Mater Interfaces*. 2017;9(18):15328–15341.
18. Rizzello L, Pompa PP. Nanosilver-based antibacterial drugs and devices: mechanisms, methodological drawbacks, and guidelines. *Chem Soc Rev*. 2014;43(5):1501–1518.
19. Wang Z, Xia T, Liu S. Mechanisms of nanosilver-induced toxicological effects: more attention should be paid to its sublethal effects. *Nanoscale*. 2015;7(17):7470–7481.
20. Ordzhonikidze CG, Ramaiyya LK, Egorova EM, Rubanovich AV. Genotoxic effects of silver nanoparticles on mice in vivo. *Acta Naturae*. 2009;1(3):99–101.
21. Kim JS, Sung JH, Ji JH, et al. In vivo genotoxicity of silver nanoparticles after 90-day silver nanoparticle inhalation exposure. *Saf Health Work*. 2011;2(1):34–38.
22. Stebounova LV, Adamcakova-Dodd A, Kim JS, et al. Nanosilver induces minimal lung toxicity or inflammation in a subacute murine inhalation model. *Part Fibre Toxicol*. 2011;8(1):5.
23. Recordati C, De Magile M, Bianchessi S, et al. Tissue distribution and acute toxicity of silver after single intravenous administration in mice: nano-specific and size-dependent effects. *Part Fibre Toxicol*. 2015;13:12.
24. Murphy A, Casey A, Byrne G, Chambers G, Howe O. Silver nanoparticles induce pro-inflammatory gene expression and inflammasome activation in human monocytes. *J Appl Toxicol*. 2016;36(10):1311–1320.
25. Alexander JW. History of the medical use of silver. *Surg Infect (Larchmt)*. 2009;10(3):289–292.
26. Liu M, Fang F, Song X, et al. The first visually observable three-mode antibiotic switch and its relative 3D printing assisted applications. *J Mater Chem B*. 2016;4(15):2544–2547.
27. Morishita Y, Yoshioka Y, Takimura Y, et al. Distribution of silver nanoparticles to breast milk and their biological effects on breast-fed offspring mice. *ACS Nano*. 2016;10(9):8180–8191.
28. Kwok KW, Dong W, Marinakos SM, et al. Silver nanoparticle toxicity is related to coating materials and disruption of sodium concentration regulation. *Nanotoxicology*. 2016;10(9):1306–1317.
29. Zeng JB, Fan SG, Zhao CY, et al. A colorimetric agarose gel for formaldehyde measurement based on nanotechnology involving Tollens reaction. *Chem Commun (Camb)*. 2014;50(60):8121–8123.
30. Rittirsch D, Huber-Lang MS, Flierl MA, Ward PA. Immunodesign of experimental sepsis by cecal ligation and puncture. *Nat Protoc*. 2009;4(1):31–36.
31. Samberg ME, Oldenburg SJ, Monteiro-Riviere NA. Evaluation of silver nanoparticle toxicity in skin in vivo and keratinocytes in vitro. *Environ Health Perspect*. 2010;118(3):407–413.
32. Kawata K, Osawa M, Okabe S. In vitro toxicity of silver nanoparticles at noncytotoxic doses to HepG2 human hepatoma cells. *Environ Sci Technol*. 2009;43(15):6046–6051.

Supplementary materials

Table S1 Zeta potentials of Ag-C with different NaCl concentrations

	Ag-C	Ag-C+1×NaCl	Ag-C+2×NaCl	Ag-C+4×NaCl	Ag-C+8×NaCl	Ag-C+10×NaCl
Zeta potentials (mV)	−72.39±1.76	−80.78±4.15	−67.66±1.3	−52.12±6.81	−48.36±1.37	−42.09±3.46

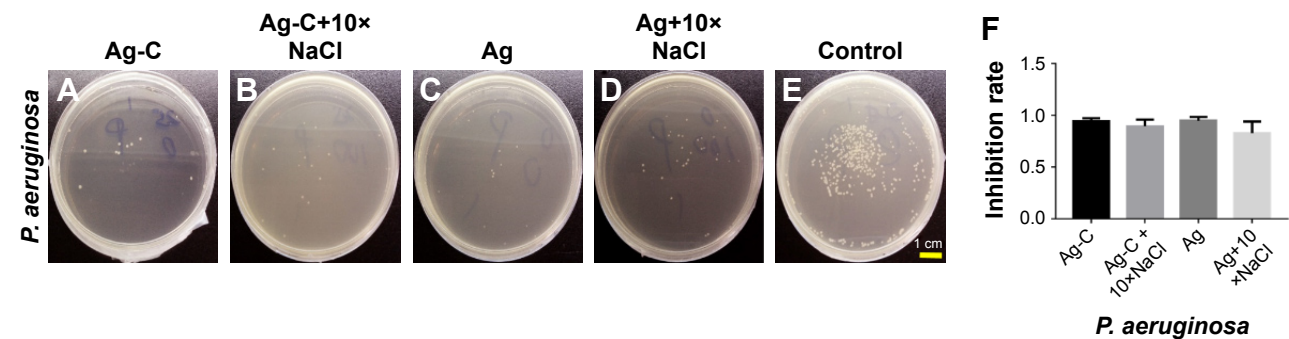**Abbreviation:** Ag-C, carbon membrane packaged Ag nanoparticles.

Figure S1 Plate counting photographs.

Notes: Gram-negative *Pseudomonas aeruginosa* co-cultured with Ag-C and Ag alone or with 10× NaCl in vitro for 3 h (**A–E**). The corresponding inhibition rates of the formulations with the bacteria, respectively (**F**). There were no statistical differences between groups.

Abbreviation: Ag-C, carbon membrane packaged Ag nanoparticles.
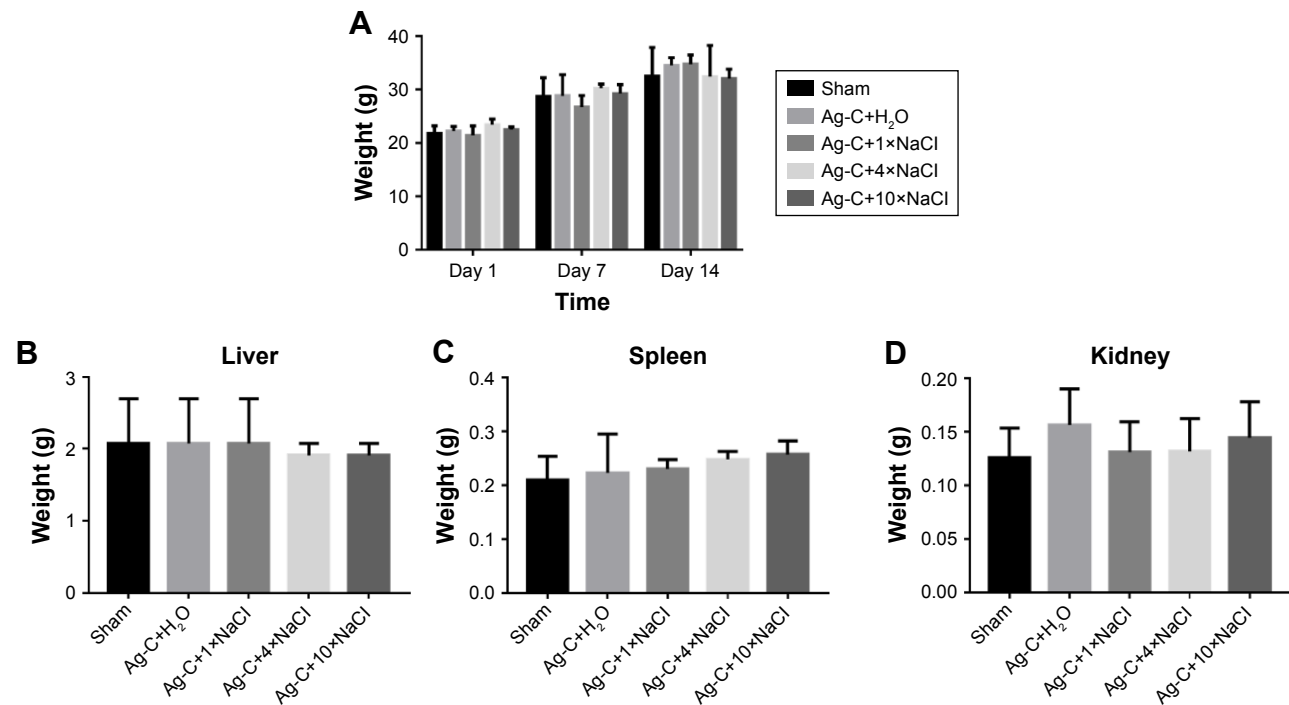
Figure S2 (*Continued*)
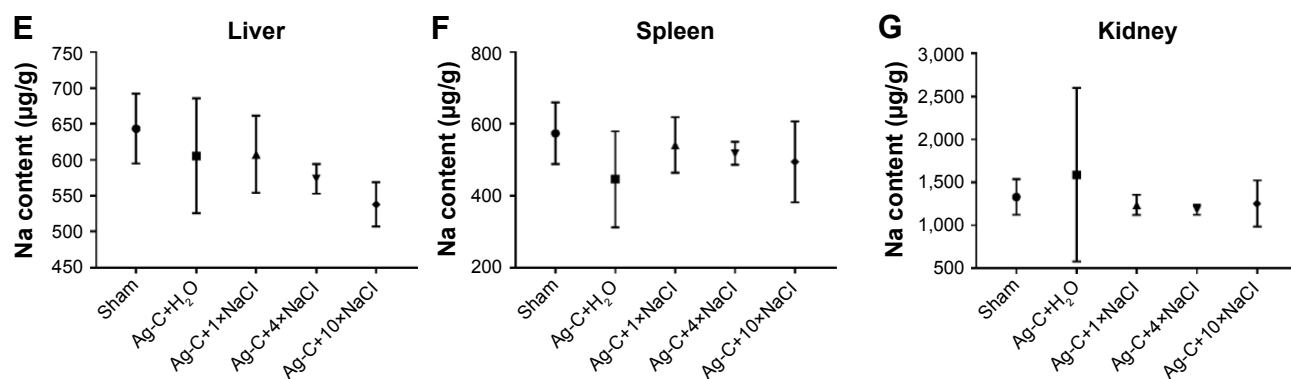
Figure S2 Body and organ weight.
Notes: Body and organ weight after treatment with Ag-C and different concentrations of NaCl under normal conditions (**A–D**). The average content of Na to each mouse in different tissues was analyzed (**E–G**). There were no statistical differences between groups.
Abbreviation: Ag-C, carbon membrane packaged Ag nanoparticles.
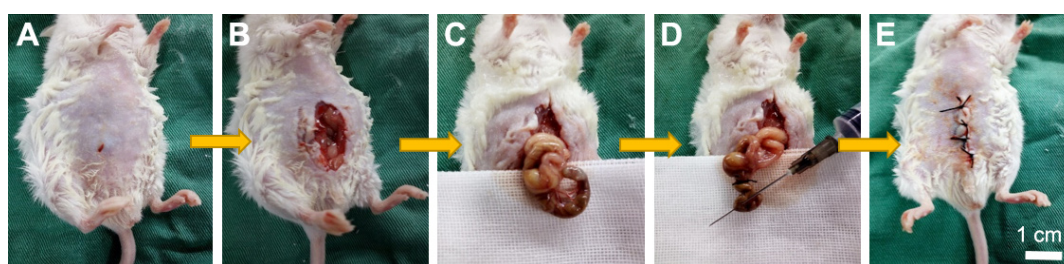
Figure S3 Critical steps in the CLP procedure in mice (**A–E**).
Abbreviation: CLP, cecal ligation and puncture.